

# Synthesis and characterization of Zn/ZnO microspheres on indented sites of silicon substrate

NASAR AHMED<sup>1,\*</sup>, ABDUL MAJID<sup>1,2</sup>, M.A. KHAN<sup>1</sup>, M. RASHID<sup>1</sup>, Z.A. UMAR<sup>3</sup>, M.A. BAIG<sup>1,3</sup>

<sup>1</sup>Department of Physics, University of Azad Jammu and Kashmir, Muzaffarabad-13100, Pakistan

<sup>2</sup>Department of Physics, College of Science, Majmaah University, P.O. Box no. 1712, Al-Zulfi 11932, Saudi Arabia

<sup>3</sup>National Centre for Physics, Quaid-i-Azam University Campus, 45320 Islamabad, Pakistan

Self-assembled Zn/ZnO microspheres have been accomplished on selected sites of boron doped P-type silicon substrates using hydrothermal approach. The high density Zn/ZnO microspheres were grown on the Si substrates by chemical treatment in mixed solution of zinc sulfate  $ZnSO_4 \cdot 7H_2O$  and ammonium hydroxide  $NH_4(OH)$  after uniform heating at 95 °C for 15 min. The Zn/ZnO microspheres had dimensions in the range of 1  $\mu m$  to 20  $\mu m$  and were created only on selected sites of silicon substrate. The crystal structure, chemical composition and morphology of as-prepared samples were studied by using scanning electron microscope SEM, X-ray diffraction XRD, energy dispersive X-ray spectroscopy EDS, Fourier transform infrared spectroscopy FT-IR and UV-Vis diffuse reflectance absorption spectra DRS. The energy band gap  $E_g$  of about 3.28 eV was obtained using Tauc plot. In summary, this study suggests that interfacial chemistry is responsible for the crystal growth on indented sites of silicon substrate and the hydrothermal based growth mechanism is proposed as a useful methodology for the formation of highly crystalline three dimensional (3-D) Zn/ZnO microspheres.

Keywords: Zn/ZnO; hydrothermal synthesis; microspheres; growth; indent

## 1. Introduction

The fabrication and synthesis of nanostructured materials have much importance because of their potential applications in various fields of fundamental and applied research. Among all micro- and nanostructured materials, zinc oxide has attracted remarkable attention of many researchers. Zinc oxide is piezoelectric, direct and wide band gap (3.39 eV) semiconductor material. It has a wide range of applications in electronics, optoelectronics, electrochemistry and electromechanical devices, such as ultraviolet lasers, light-emitting diodes, field emission devices, high performance nanosensors solar cells, piezoelectric nanogenerators, and nanopiezotronics [1]. ZnO tends to grow anisotropically into non spherical structures due to its hexagonal wurtzite structure. Large number of potential applications in photonics,

drug delivery and catalysis can be obtained by controlling the morphology of self-assembled micro/nanostructures of ZnO.

Numerous efforts have been made for controlled fabrication and synthesis of three dimensional ZnO microstructures. In recent decades, researchers found that 2-D nanosheets and 3-D microspheres have advantages over 1-D nanomaterials in electronics and photocatalysis. The unique properties of ZnO depend on the size and the morphology of particles [2–5]. At micron or submicron (nano) levels, these properties also depend on the synthesis technique as well as the reaction parameters. The main objective of researchers is to fabricate the ZnO structures with tunable properties and desired morphology. Various ZnO nanostructures, such as nanowires [6–11], nanorods [12–16], tetrapods [17–19] and nanoribbons/belts [20–22], were synthesized using different methods, such as chemical vapor deposition [4, 23], electrodeposition [24], laser ablation [25], physical

\*E-mail: nasar.ahmed@ajku.edu.pk

vapor deposition, molecular beam epitaxy MBE, sputtering, flux methods, electrospinning, thermal oxidation [27] and hydrothermal/solvothermal synthesis [2, 5, 11–14, 25–29]. Synthesis of 2D and 3D ZnO nanomaterials, characterization and investigation of their properties is an important field of research [23, 26, 30–33]. Furthermore, the hydrothermal method has become a recent trend for the fabrication of metal oxides.

In the present paper, we have used the hydrothermal synthesis method to study the growth mechanism of three-dimensional Zn/ZnO microspheres. The hydrothermal technique has advantages of limited tendency of particles to aggregate along with high homogeneity of crystalline structure and morphology. Moreover, the hydrothermal method is an environmental friendly technique because it does not require organic solvents or additional processing of the product [34]. In the present work, we report the hydrothermal synthesis method for the fabrication of self-assembled Zn/ZnO microspheres on a boron doped P-type pre-indented silicon substrate along with its characterization.

## 2. Experimental

### 2.1. Synthesis of ZnO microspheres

Solution of zinc sulfate  $\text{ZnSO}_4 \cdot 7\text{H}_2\text{O}$  (BdH) with deionized water (DI) was prepared using magnetic stirrer until all the zinc sulfate was completely dissolved. The optimized quantities of zinc sulfate  $\text{ZnSO}_4 \cdot 7\text{H}_2\text{O}$  (BdH) and ammonium hydroxide  $\text{NH}_4(\text{OH})$  (Fisher Scientific, 99.9 %) were mixed and dissolved to get the molar ratio of  $\text{Zn}^{2+}/\text{NH}_3$  of about 1:10. A cleaned laser indented piece (1 cm  $\times$  1 cm) of boron doped p-type silicon (1 1 1) (MTI Corporation, USA) was placed in a flask containing solution of  $\text{Zn}^{2+}/\text{NH}_3$ , and 1.0 g of pure zinc powder (BdH) was added into the solution. The entire system was transferred to an oven for uniform heating at around 95 °C for 15 min and then the sample was allowed to cool down to room temperature. The prepared sample was washed by dipping it in deionized (DI) water and dried in air at 150 °C for 5 min. Finally, the as-prepared sample was characterized using scanning electron

microscope SEM. The size of Zn/ZnO microspheres was determined by SEM, the structural properties were characterized by X-ray diffraction XRD, composition of prepared sample was studied by the energy dispersive X-ray spectroscopy EDX. In addition, optical properties were studied by ultraviolet visible infrared spectroscopy UV-Vis-IR and the Fourier transform infrared spectroscopy FT-IR was used to identify the rotational and vibrational modes present within the structure. These studies indicated the formation of three dimensional Zn/ZnO microspheres on selected sites of the silicon substrate by simple hydrothermal route.

### 2.2. Characterization techniques

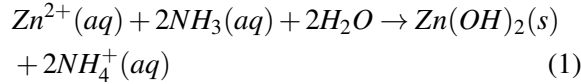
The topography of the prepared sample was studied by scanning electron microscope (Jeol JSM-6510LV) and the size of observed microspheres was found to be between 1  $\mu\text{m}$  to 20  $\mu\text{m}$ . The structural properties were characterized by X-ray diffraction (PANalytical X'Pert Pro system) and the sample was scanned in the continuous mode from 5° to 80°. The energy dispersive X-ray spectrometer (EDX-Oxford X-Act analytical silicon drift detector) attached to SEM was used to study the structure of Zn/ZnO microspheres. The UV-Vis absorption spectrum of Zn/ZnO microspheres was recorded by the PerkinElmer Lambda 950 spectrophotometer covering the wavelength range of 350 nm to 480 nm and the optical properties of the produced Zn/ZnO microspheres were studied. In addition, the Fourier transform infrared spectrum (PerkinElmer 100 FT-IR spectrometer) was also recorded to confirm the purity of fabricated material.

## 3. Results and discussion

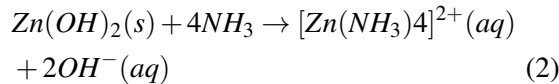
### 3.1. Growth mechanism of Zn/ZnO microspheres

The growth mechanism of the Zn/ZnO microspheres can be described by the hydrothermal approach. Initially, zinc sulfate  $\text{ZnSO}_4 \cdot 7\text{H}_2\text{O}$  dissociates in water to produce zinc ( $\text{Zn}^{2+}$ ) and sulfate ions ( $\text{SO}_4^{2-}$ ). The addition of ammonia

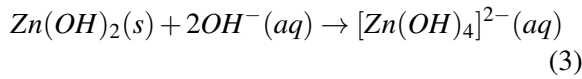
(NH<sub>3</sub>) changes the pH of the solution and produces white gelatinous Zn(OH)<sub>2</sub> precipitate due to the reaction of zinc (Zn<sup>2+</sup>) ion with aqueous ammonia:



After adding ammonium hydroxide in an excess amount, zinc complexes start to develop. The precipitates start to dissolve in solution and the solution turns clear when the molar ratio of Zn<sup>2+</sup>/NH<sub>3</sub> reaches 1:4 or higher:



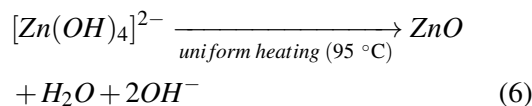
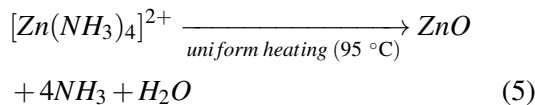
It is also equally possible that Zn(OH)<sub>2</sub> reacts with the excess hydroxyl ions to produce [Zn(OH)<sub>4</sub>]<sup>2-</sup>:



The concentration of [OH]<sup>-</sup> plays an important role in the controlled growth of different crystal faces and pH ≥ 10 provides a suitable environment for the formation of complexes [35]. At higher temperature, complex solution forms the zinc hydroxide:



Upon heating at 95 °C, zinc complexes dissociate and dehydrate to form ZnO:



Further addition of zinc produces Zn/ZnO composite structures and forms Zn/ZnO nanostructures in the solution. This solution supersaturated with the Zn/ZnO nanostructures possesses a high Gibbs free energy; the overall energy of the system reduces by segregation of solute from the solution.

This reduction of Gibbs free energy is the driving force for both nucleation and growth. The surface binding energy at indented sites is increased due to the defects and counterbalanced by reduction of this energy at the indented sites, which is accompanied by the formation of a new phase [36]. Due to this fact Zn/ZnO microspheres grow only at indented sites.

SEM images in Fig. 1 confirm the growth of Zn/ZnO microspheres with varying diameter within 1 μm to 20 μm and all generated Zn/ZnO microspheres are nearly spherical in shape. Fig. 1a shows the formation of Zn/ZnO microspheres on the indented sites and the white circle shows the area enclosing the indented portion. It is also clear from the image that the indents formed by laser exhibit a uniform spherical shape. Fig. 1b and Fig. 1c show that Zn (small particles are zinc because we added nanosize zinc particles) is also present along with ZnO (large spheres) and these images also confirm that Zn/ZnO composite microspheres were grown only at indented sites of silicon substrate. Fig. 1d and Fig. 1e show the enlarged view of microspheres where the particles were formed by nanograins. It is pertinent to mention here that with an increase in the resolution of SEM, gradual changes in size and surface of microspheres are observed and they reveal a rough surface. Fig. 1f depicts the morphology of irregular shaped pure Zn with approximate diameter of 5 μm. Fig. 1g and Fig. 1h show the highly magnified SEM images of microspheres.

### 3.2. Structural characterization of Zn/ZnO microspheres

The XRD spectrum, as shown in Fig. 2, reveals the prominent peaks of hexagonal ZnO belonging to (1 0 0), (0 0 2), (1 0 1), (2 0 1) phases along with the weak phases of (1 1 0), (1 0 3) and (2 0 2). However, few peaks of Zn belonging to (1 0 0), (1 0 1), (1 0 2), (1 0 3) and Zn (1 1 0) phases have also appeared. It is observed from the recorded spectrum that the structure is composed of wurtzite ZnO and the characteristic peaks of Zn/ZnO microspheres are found to be in good agreement with those of the standard patterns

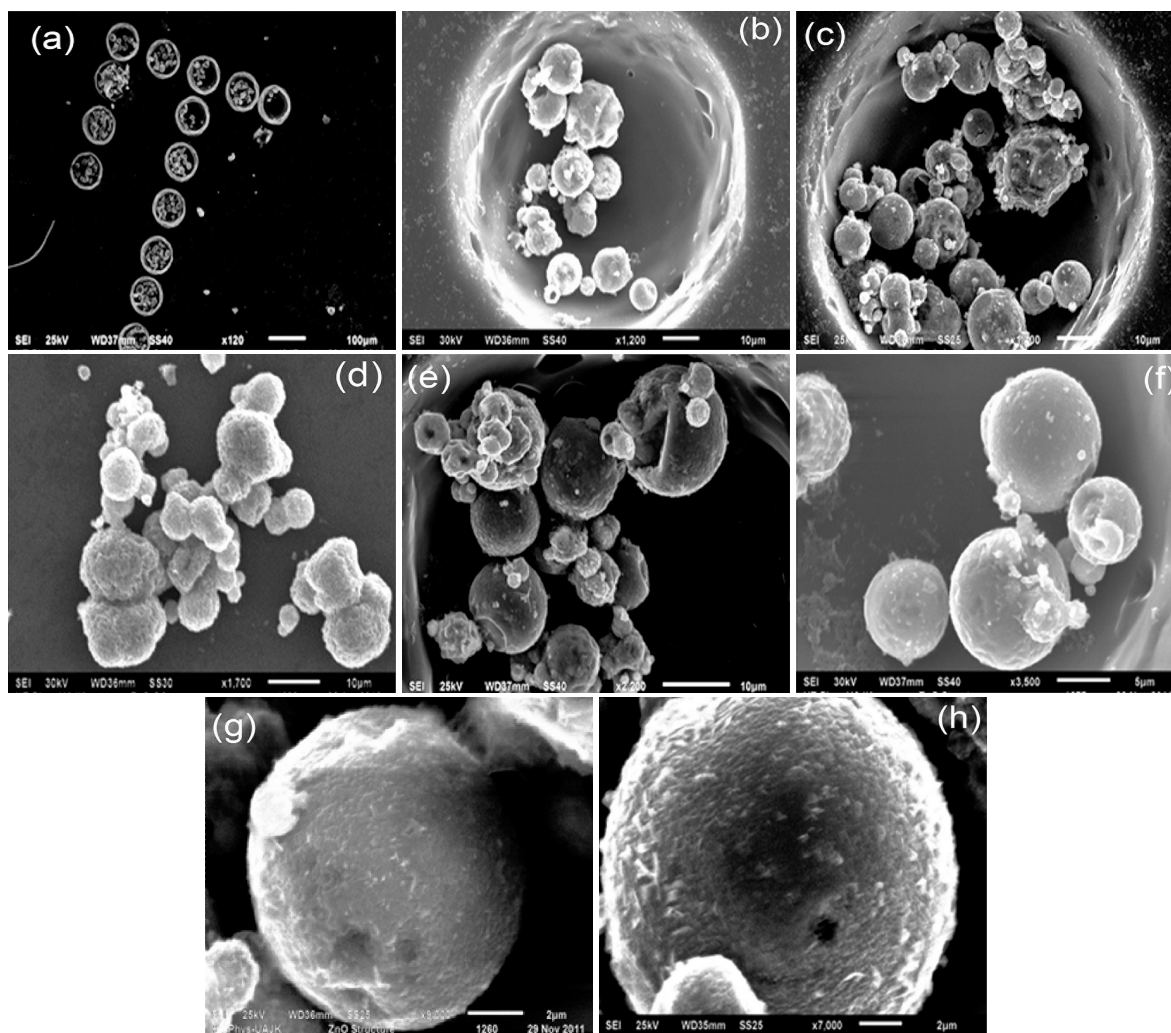


Fig. 1. (a) low magnification SEM image of Zn/ZnO microspheres only on indented sites of silicon substrate. (b) and (c) SEM images of Zn/ZnO microspheres successfully grown on the indented sites (d) to (h) high magnification SEM images of Zn/ZnO microspheres.

of hexagonal wurtzite ZnO structure. In addition, the recorded peak positions and relative intensities of Zn/ZnO microspheres are comparable with the reported values from JCPDS Card No. 00-036-1451 for ZnO and JCPDS PDF# 00-004-0831 for Zn [37]. The diffraction peaks of Zn are also seen in the XRD spectrum and these peaks confirm high crystallinity of the structures [38]. The Zn peak further confirms the formation of Zn/ZnO composite.

The crystallite size of the ZnO has been calculated by using the Debye-Scherrer formula [39, 40]:

$$\text{Crystallite size} = \frac{0.9\lambda}{FWHM \cos\theta} \quad (7)$$

where the value of  $\lambda$  (wavelength of the X-ray) is 0.154 nm, FWHM is the full width at half maximum of the diffraction peak, and  $\theta$  is the Bragg angle. The estimated average crystallite size of ZnO microspheres is calculated about 1  $\mu\text{m}$ .

The calculated lattice constants and unit volume cell (shown in Table 1) for the wurtzite ZnO determined from the XRD analysis are in good agreement with the theoretical calculations. The minor

Table 1. Calculated and standard lattice parameters.

ZnO	a [Å]	c [Å]	Wurtzite c/a	Unit cell volume
Standard	3.2498	5.2066	1.6021	47.62
Calculated	3.2725	5.2314	1.5986	48.51

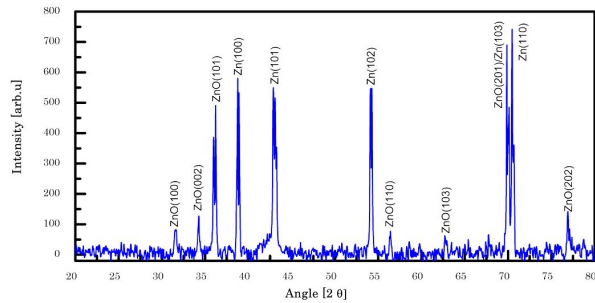


Fig. 2. XRD peaks of Zn/ZnO microspheres grown on indented sites.

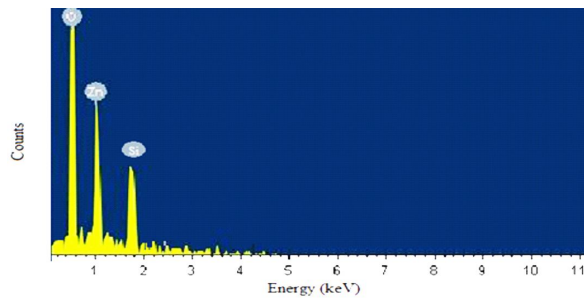


Fig. 3. EDS Zn/ZnO microspheres obtained by hydrothermal route.

deviation in the calculated and the ideal wurtzite crystal values is observed which may be due to the lattice stability and ionicity [41]. Özgür et al. [41] suggested that the point defects, such as zinc antisites, oxygen vacancies, and extended defects, such as threading dislocations, result in the increase in the lattice constant.

### 3.3. Compositional analysis of Zn/ZnO microspheres

Energy dispersive spectroscopy EDS system attached to the SEM (Oxford X-Act analytical silicon drift detector) was used to study the composition of elements present in the prepared samples. Fig. 3 shows the EDS spectrum of a prepared sample demonstrating that the sample contains only Zn,

O and Si. The prominent peaks corresponding to Zn and O confirm that the sample contains ZnO. The Si peak observed in the spectrum comes from the Si substrate [35]. No other peak corresponding to any other element has been detected. The atomic and weight percentages of the detected elements are listed in Table 2.

Table 2. Atomic and percentage weight of the zinc, oxygen and silicon obtained from EDX.

Element	Weight [%]	Atomic [%]
Si K	6.58	8.70
Zn L	71.53	40.58
O	21.88	50.72

### 3.4. Optical properties of Zn/ZnO microspheres

UV-Vis absorption spectroscopy was used to study the optical properties of the Zn/ZnO microspheres. UV-Vis absorption spectrum of the Zn/ZnO microspheres measured at room temperature is shown in Fig. 4. A prominent excitation band at 378 nm corresponding to the ZnO nanograins is clearly seen. This absorption peak represents a red shift as compared to the bulk exciton absorption of ZnO (373 nm) [42] which is due to the size effect. The absorption near the visible range implies that there exist some defect energy levels in the synthesized Zn/ZnO microspheres that may be due to the specific experimental synthesis conditions [43].

The Tauc plot is used to determine the optical band gap  $E_g$  of prepared structures [44] as shown in Fig. 5. Here, the absorption coefficient  $\alpha$  is a function of the incident photon energy and optical band gap as given by the relation:

$$\alpha = \frac{A(h\nu - E_g)^{\frac{1}{2}}}{h\nu} \quad (8)$$

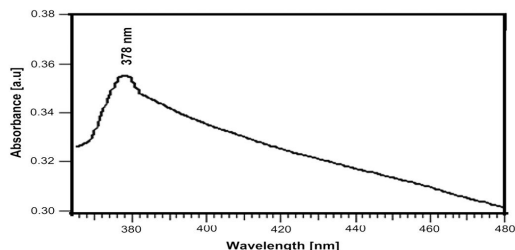


Fig. 4. UV-Vis absorption spectrum of Zn/ZnO microspheres.

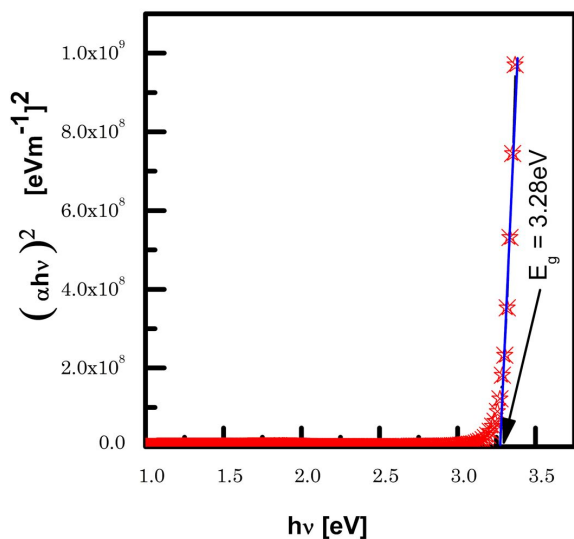


Fig. 5. Band gap calculation using Tauc plot.

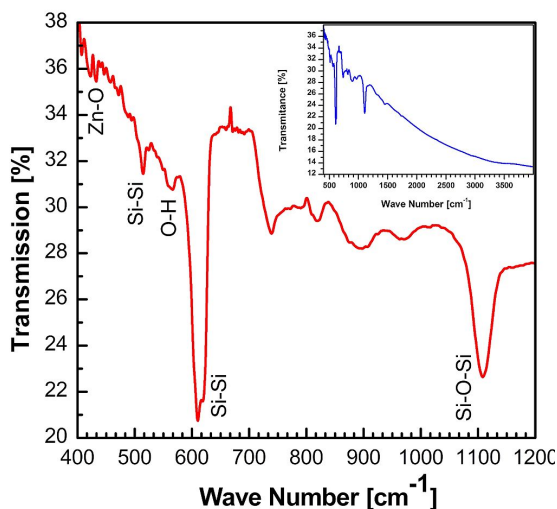


Fig. 6. FT-IR spectrum of the prepared samples.

where  $\alpha$  is absorption coefficient,  $h$  is the Planck constant,  $\nu$  is the frequency of vibration,  $E_g$  is the band gap and  $A$  is the proportionality constant. The energy band gap  $E_g$  of about 3.28 eV has been obtained from the intercept of the extrapolated linear part of the curve which is due to the size effect.

### 3.5. Fourier transform infrared (FT-IR) spectroscopy

Fig. 6 shows the FT-IR spectrum of the Zn/ZnO composite microspheres. The inset in Fig. 6 shows the full range spectrum in the range of  $400\text{ cm}^{-1}$  to  $4000\text{ cm}^{-1}$  with the enlarged spectrum between  $400\text{ cm}^{-1}$  and  $1200\text{ cm}^{-1}$ . A series of absorption peaks corresponding to Si and ZnO is clearly observed in the enlarged spectrum in the range of  $400\text{ cm}^{-1}$  to  $1200\text{ cm}^{-1}$ . The peaks at  $514\text{ cm}^{-1}$  and  $610\text{ cm}^{-1}$  are related to Si. The absorption peak of Si is also observed for the interstitial oxygen at  $1107\text{ cm}^{-1}$ . The absorption peaks at  $566\text{ cm}^{-1}$  are assigned to O–H bonding of the hydroxyl group and Zn–O stretching of ZnO at  $432\text{ cm}^{-1}$  [45–50].

## 4. Conclusions

Using hydrothermal route, we have successfully grown and characterized Zn/ZnO microspheres on the boron doped P-type silicon substrates only on the indented sites of the substrate. The size and morphology of the prepared samples was characterized by SEM and the microspheres were found to have micrometer dimensions (their diameter ranged from  $1\text{ }\mu\text{m}$  to  $20\text{ }\mu\text{m}$ ). Moreover, the experimental results of the SEM studies evidenced that the growth took place only on the indented parts. The structure of the Zn/ZnO microspheres was characterized using XRD and the sharp peaks of Zn/ZnO microspheres in the recorded spectrum were assigned to the hexagonal wurtzite structure of ZnO, which is one of the most stable structures of this material. Energy dispersive spectroscopy EDX confirmed that the prepared structures contain ZnO because of the prominent peaks belonging to Zn and O in the recorded spectrum. UV-Vis spectroscopy was carried out to study the optical properties of the Zn/ZnO microspheres. It was revealed

that a prominent exciton band at 378 nm corresponds to the ZnO nanograins. Finally, FT-IR spectrum provided information about the stretching and vibrational modes of the bonds present in the prepared samples. The silicon peaks observed in the EDX and FT-IR spectra are due to the presence of silicon substrate. In summary, this study shows that hydrothermal route can be used for the growth of highly crystalline three dimensional Zn/ZnO structures on a silicon substrate in numerous applications such as drug delivery, optoelectronics, UV and blue light LEDs.

### Acknowledgements

We are grateful to the Higher Education Commission of Pakistan for the indigenous PhD scholarship to Nasar Ahmed.

### References

- [1] MENDE L.S., DRISCOLL J.L., *Mater. Today*, 10 (2007), 40.
- [2] LIANG J., LIU J., XIE Q., BAI S., YU W., QIAN Y., *Phys. J. Chem. B*, 109 (2005), 9463.
- [3] LIU X., *Angew. Chem. Int. Edit.*, 48 (2009), 3018.
- [4] WANG H., XIE C., ZENG D., *Cryst. J. Growth*, 277 (2005), 372.
- [5] LU F., CAI W., ZHANG Y., *Adv. Funct. Mater.*, 18 (2008), 1047.
- [6] HUANG M.H., MAO S., FEICK H., YAN H., WU Y., KIND H., WEBER E., YANG P., *Science*, 292 (2001), 1897.
- [7] HUANG M.H., WU Y., FEICK H., TRAN N., WEBER E., YANG P., *Adv. Mater.*, 13 (2001), 113.
- [8] YAO B.D., CHAN Y.F., WANG N., *Phys. Lett.*, 81 (2002), 757.
- [9] GREENE L.E., LAW M., TAN D.H., MONTANO M., GOLDBERGER J., SOMORJAI G., YANG P., *Nano Lett.*, 5 (2005), 1231.
- [10] LIU C.H., ZAPIEN J.A., YAO Y., MENG X.M., LEE C.S., FAN S.S., LIFSHITZ Y., LEE S.T., *Adv. Mater.*, 15 (2003), 838.
- [11] LI S.Y., LIN P., LEE C.Y., TSENG T.Y., *J. Appl. Phys.*, 95 (2004) 3711.
- [12] LIU B., ZENG H.C., *J. Am. Chem. Soc.*, 125 (2003), 4430.
- [13] GAO X.P., ZHENG Z.F., ZHU H.Y., PAN G.L., BAO J.L., WU F., SONG D.Y., *Chem. Commun.*, 1 (2004), 1428.
- [14] PARK W.I., JUN Y.H., JUNG S.W., YI G.C., *Appl. Phys. Lett.*, 82 (2003), 964.
- [15] HARTANTO A.B., NING X., NAKATA Y., OKADA T., *Appl. Phys. A*, 78 (2003), 299.
- [16] YU W.D., LI X.M., GAO X.D., *Appl. Phys. Lett.*, 84 (2004), 2658.
- [17] DAI Y., ZHANG Y., LI Q.K., NAN C.W., *Chem. Phys. Lett.*, 358 (2003), 83.
- [18] DAI Y., ZHANG Y., WANG Z.L., *Solid State Commun.*, 126 (2003), 629.
- [19] ROY V.A.L., DJURIŠIĆ A.B., CHAN W.K., GAO J., LUI H.F., SURYA C., *Appl. Phys. Lett.*, 83 (2003), 141.
- [20] PAN Z.W., DAI Z.R., WANG Z.L., *Science*, 291 (2001), 1947.
- [21] YAN H., JOHNSON J., LAW M., HE R., KNUTSEN K., MCKINNEY J.R., PHAM J., SAYKALLY R., YANG P., *Adv. Mater.*, 15 (2003), 1907.
- [22] LI Y.B., BANDO Y., SATO T., KURASHIMA K., *Appl. Phys. Lett.*, 81 (2002), 144.
- [23] SULIEMAN K.M., HUANG X.T., LIU J.P., TANG M., *Nanotechnology*, 17 (2006), 4950.
- [24] WANG Y.L., BOUCHAIB S., BROURI T., CAPOCHICHI M., LAURENT K., LEOPOLDES J., TUSSEAU-NENEZ S., LEI L., CHEN Y., *Mater. Sci. Eng. B-Adv.*, 170 (2010), 107.
- [25] YU W.D., LI X.M., GAO X.D., *Appl. Phys. Lett.*, 84 (2004), 2658.
- [26] XU J., FAN K., SHI W., LI K., PENG T., *Sol. Energy*, 101 (2014), 150.
- [27] LI P., WEI Y., LIU H., WANG X., *Solid State Chem.*, 178 (2005), 855.
- [28] MCBRIDE R.A., KELLY J.M., MCCORMACK D.E., *J. Mater. Chem.*, 13 (2003), 1196.
- [29] LEDWITH D., PILLAI S.C., WATSON G.W., KELLY J.M., *Chem. Commun.*, 01 (2004), 2294.
- [30] CHEN S.J., LIU Y.C., SHAO C.L., MU R., LU Y.M., ZHANG J.Y., SHEN X.D.Z., FAN W., *Adv. Mater.*, 17 (2005), 586.
- [31] KISAILUS D., SCHWENZER B., GOMM J., WEAVER J.C., MORSE D.E., *Am J. Chem. Soc.*, 28 (2006), 10276.
- [32] ÖZGÜR Ü., ALIVOV Y.I., LIU C., TEKE A., RESHCHIKOV M.A., DOĞAN S., AVRUTIN V., CHO S.J., MORKOÇ H., *J. Appl. Phys.*, 98 (2005), 041301.
- [33] ZHU Y.F., FAN D.H., SHEN W.Z., *J. Phys. Chem. C*, 111 (2007), 18629.
- [34] RADZIMSKA A.K., JESIONOWSKI T., *Materials*, 7 (2014), 2833.
- [35] LUPAN O., CHOW L., CHAI G., HEINRICH H., *Chem. Phys. Lett.*, 465 (2008), 249.
- [36] MARTIN P.M., *Deposition Technologies for films and coatings*, Science & Technology, Elsevier, 2010.
- [37] Joint Committee on Powder Diffraction Standards, Powder Diffraction File No 036-1451 and #00-004-0831.
- [38] LEE C.Y., TSENG T.Y., LI S.Y., LIN P., TAMKAN G., *J. Sci. Eng.*, 6 (2003), 127.
- [39] CULLITY B.D., STOCK S.R., *Elements of X-ray diffraction*, Prentice-Hall, 3<sup>rd</sup> ed., New Jersey, 2001, p. 388.
- [40] UMAR Z.A., AHMED N., AHMED R., ARSHAD M., ANWAR M., HUSSAIN T., BAIG M.A., *Surf. Interface Anal.*, 50 (3) (2018), 297.

- [41] ÖZGÜR U., ALIVOV Y.I., LIU C., TEKE A., RESHCHIKOV M.A., DOGAN S., AVRUTIN V., CHO S.J., MORKOÇ H., *J. Appl. Phys.*, 98 (2005), 041301.
- [42] ZHENG H., MEI Z.X., ZENG Z.Q., LIU Y.Z., GUO L.W., JIA J.F., XUE Q.K., ZHANG Z., DU X.L., *Thin Solid Films*, 520 (2011) 445.
- [43] SINGH S.C., SWARNKAR R.K., GOPAL R., *B. Mater. Sci.*, 33 (2010), 21.
- [44] TAUC J., GRIGORVICI R., YANCA Y., *Phys. Status Solidi A*, 15 (1966), 627.
- [45] ZHU J.J., AALTONEN T., VENKATACHALAPATHY V., GALECKAS A., KUZNETSOV YU A., *The 14<sup>th</sup> International Conference on Metalorganic Vapor Phase Epitax.* 310 (2008), 5020.
- [46] SUWANBOON S., *Science Asia*, 34 (2008), 031.
- [47] VÁSQUEZ M.A., RODRÍGUEZ G.A., GARCÍA-SALGADO G., ROMERO-PAREDES G., PEÑA-SIERRA R., REVISTA-MEXICANA D., *Fisica*, 53 (2007), 431.
- [48] WANG Y.X., SUN J., FAN X.Y., YU X., *Ceram. Int.*, 37 (2011), 3431.
- [49] GEETHA D., THILAGAVATHI D.T., *Nanomaterials-Basel*, 1 (2010), 297.
- [50] KATUMB G., MWAKIKUNG B.W., MOTHIBINYANE T.R., *Nanoscale Res. Lett.*, 3 (2008), 421.

Received 2017-10-13

Accepted 2018-05-07